A Bidirectional Control Principle of Active Tuned Hybrid Power Filter Based on the Active Reactor Using Active Techniques

Yaping Deng, Xiangqian Tong, and Hao Jia

***Abstract*—In this paper, a novel bidirectional control principle of active tuned hybrid power filter (ATHPF) based on the active reactor using active techniques is proposed. The proposed control principle, in essence, is to continuously adjust the filter inductance of the active reactor by regulating active power filter (APF) output current in terms of its magnitude and direction. Therefore, the ATHPF using the bidirectional control principle can simultaneously supply different impedances at different selective suppressed harmonic frequencies. The bidirectional control principle can perform both the normal active tuning function and the abnormal active detuning function. To be specific, the normal active tuning function refers to the harmonic elimination with filtering performance independent of the deviation of passive filter parameters, while the latter, the abnormal active detuning function, refers to the flexible protection against harmonic over-current without losing two harmonic elimination and reactive power compensation at the occurrence of harmonic over-current. Experimental results verify the effectiveness of the ATHPF with the bidirectional control principle in selective harmonic elimination and flexible protection against harmonic over-current.**

***Index Terms*—Active detuning, active tuning, bidirectional control, harmonic suppression, hybrid power filter, over-current protection, power quality.**

I. Introduction

DUE TO THE increasing application of renewable generation and other power electronic equipments such as diode rectifiers and adjustable speed drives, harmonic pollution has become a critical problem in power system [1], [2]. It degrades the power quality and power supply reliability. Therefore, it is essential to install a power filter for harmonic elimination. Passive power filter (PPF) is a cost-effective approach for both harmonic elimination and power factor improvement in high-voltage power system [3]. However, it still has some inherent defects, including series/parallel resonance, filter detuning, fixed frequency, and so on [4]. Among these defects, the filter detuning caused by the deviation of system frequency and filter capacitance or inductance is a major problem [5]. It decreases the filtering effectiveness and may cause over-current of the filter. Active power filter (APF) based on power electronic techniques shows a better filtering performance than PPF [6], [7]. Nevertheless, the APF is difficult to be applied to the high-voltage power system due to its small capacity and high cost [8], [9]. Since the 1990s, several configurations of hybrid power filter have been proposed to improve the filtering performance of PPF and reduce the capacity of APF in high-voltage power system [10], [11], whereby contributing to the best effectiveness in performance/cost [12]. Among these configurations, the *LC* or C-type PPF are usually combined with APF [13]–[15]. Detjen and others have proposed a practical hybrid power filter [16], which shows great promise. In the configuration of this hybrid power filter, the APF is in parallel with the filter reactor of the *LC*-tuned filter directly or through a transformer. Therefore, the hybrid power filter can be easily used in applications with single-tuned *LC* filter already installed. Moreover, it has the advantage of small APF-rated capacity.

For hybrid power filter, control principle is quite important to achieve excellent compensation performance. Extensive control principles have been proposed to accomplish these requirements, such as resonances damping [17], harmonic current/voltage elimination [18], [19], reactive power compensation [20], and so on [21], [22]. However, these control principles are usually characterized by source current or load current detection. Therefore, it is generally recognized as a challenging task to adopt the hybrid power filter using the control principle with source current or load current information in those situations where source current or load current cannot be sensed conveniently. Thus, the hybrid power filters with source current or load current acquisition control methods are not suitable for the power system with smart grid or microgrid characterized by distributed nonlinear loads and distributed generations such as solar, wind, fuel cell, gas turbine, and so on [23], [24].

In the literature [25], an active tuning control principle has been proposed to overcome the drawbacks in the control methods with source current or load current detection. This control principle is characterized by sensing only the filter current, which is different from previous research. The filter system applying the active tuning control principle to the configuration proposed by Detjen is called active tuned hybrid power filter (ATHPF) in this paper. The ATHPF employing the active tuning control principle can achieve perfect filtering performance without source current or load current information. However, the research of ATHPF is still insufficient. In ATHPF, the main body of the filter system is still *LC* filter. As a result, when

Manuscript received January 09, 2014; revised June 16, 2014 and September 02, 2014; accepted November 17, 2014. Date of publication December 08, 2014; date of current version February 02, 2015. This work was supported in part by the Key Discipline Special Foundation of Shaanxi Province, China, under Grant 5X1301; and in part by the Specialized Research Fund for the Doctoral Program of Higher Education, China, under Grant 20126118110009. Paper no. TII-14-0024.

The authors are with the Department of Electrical Engineering, Xi'an University of Technology, Xi'an 710048, China (e-mail: xautdodo@163.com; lstong@mail.xaut.edu.cn).

Color versions of one or more of the figures in this paper are available online at http://ieeexplore.ieee.org.

Digital Object Identifier 10.1109/TII.2014.2378693

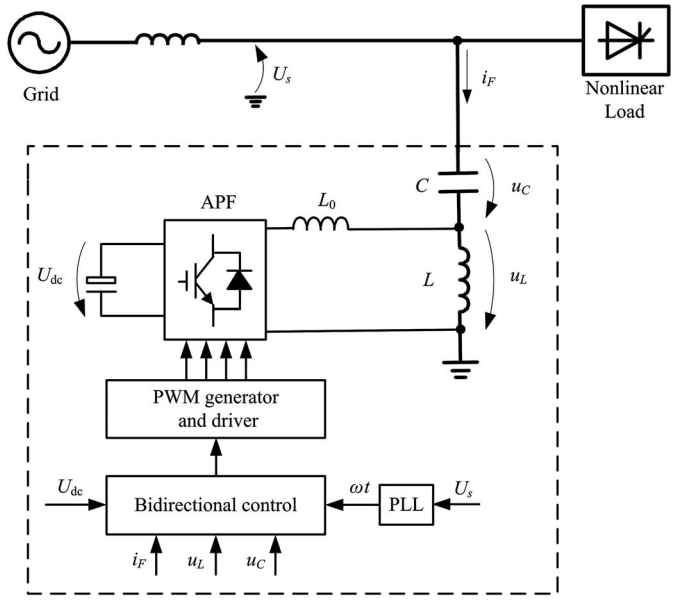

Fig. 1. Single-phase configuration of ATHPF.

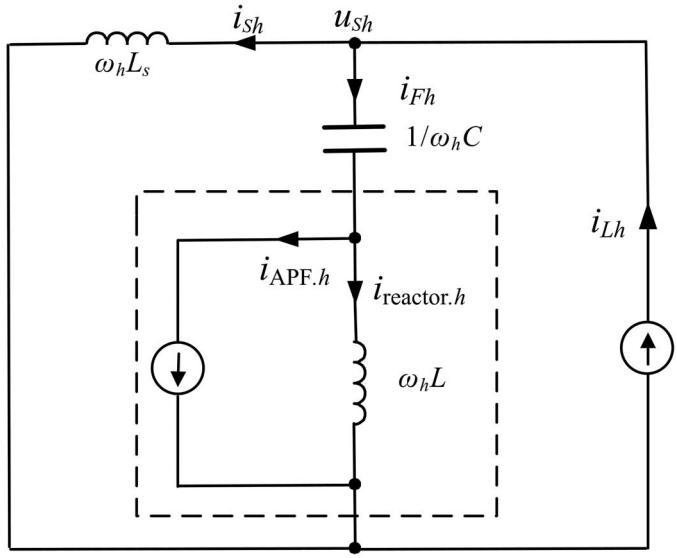

Fig. 2. h-order harmonic equivalent circuit of ATHPF.

ATHPF is well tuned at h-order harmonic frequency with the active tuning control principle, it provides low impedance path for the h-order harmonic current not only for the compensated nonlinear loads but also for the neighboring uncompensated nonlinear loads. Accordingly, the excessive harmonic current will flow into the ATHPF and lead to harmonic over-current of the filter. This will cause damage to the ATHPF. Hence, it is necessary to protect ATHPF against harmonic over-current.

On the basis of active tuning control principle, a novel bidirectional control principle is proposed in this paper to solve the problem of harmonic over-current in ATHPF. The proposed control principle can simultaneously achieve the following two goals:

1) harmonic elimination with filtering performance immune to the deviation of passive filter parameters; and
2) flexible protection against harmonic over-current without losing harmonic elimination and reactive power compensation at the occurrence of harmonic over-current.

Therefore, the operation reliability of ATHPF can be improved. The outstanding advantages of ATHPF with the bidirectional control principle become prominent especially when it is difficult to acquire the source current or load current easily. Moreover, three-phase ATHPF employing the proposed bidirectional control principle is implemented with split-phase independent control method. Consequently, the filtering performance of three-phase ATHPF is immune to the filter parameters unbalance. The experimental results have confirmed the validity of the proposed control principle in selective harmonic elimination and flexible protection against harmonic over-current.

II. System Configuration and APF Operating Principle

A. System Configuration

Fig. 1 shows the configuration of ATHPF, which is connected in parallel with nonlinear load. The filter system comprises two parts: 1) *LC* passive filter; and 2) APF with inductor L_0 to eliminate switching ripples. Since the APF, which is directly shunted to the filter reactor, only sustains very low fundamental voltage of the power system, its rated capacity is greatly reduced, which is of significant advantage to application of the hybrid power filter.

The *LC* filter in ATHPF is not necessarily designed as a well-tuned PPF because the ATHPF with the bidirectional control principle can automatically accommodate the deviation of the filter parameters. This is an important characteristic as it provides more flexibility to the parameters selection of the *LC* filter in ATHPF.

B. APF Operating Principle

Fig. 2 shows the single-phase h-order harmonic equivalent circuit of the filter system presented in Fig. 1. The nonlinear load and the APF are considered as current sources i_{Lh} and $i_{\text{APF}.h}$, respectively. The ω_h is the h-order harmonic angular frequency of power system. The $\omega_h L_S$, $\omega_h L$, and $1/\omega_h C$ are the harmonic impedances of power system, filter reactor, and filter capacitor, respectively. The u_{Sh} represents the h-order harmonic component of the source voltage. The i_{Fh} stands for the h-order harmonic current flowing into ATHPF, and the $i_{\text{reactor}.h}$ denotes the h-order harmonic current injected into the reactor L.

Based on the KCL and KVL theories, a series of formulas are obtained as follows:

$$\begin{cases} u_{Sh} = u_{Ch} + u_{Lh} \\ u_{Lh} = L\dfrac{di_{\text{reactor}.h}}{dt} \\ u_{Ch} = \dfrac{1}{C}\displaystyle\int i_{Fh}dt \\ i_{Fh} = i_{\text{reactor}.h} + i_{\text{APF}.h} \end{cases} \tag{1}$$

where C and L are the capacitance and initial inductance of the *LC* filter in ATHPF, and u_{Lh} and u_{Ch} represent the h-order

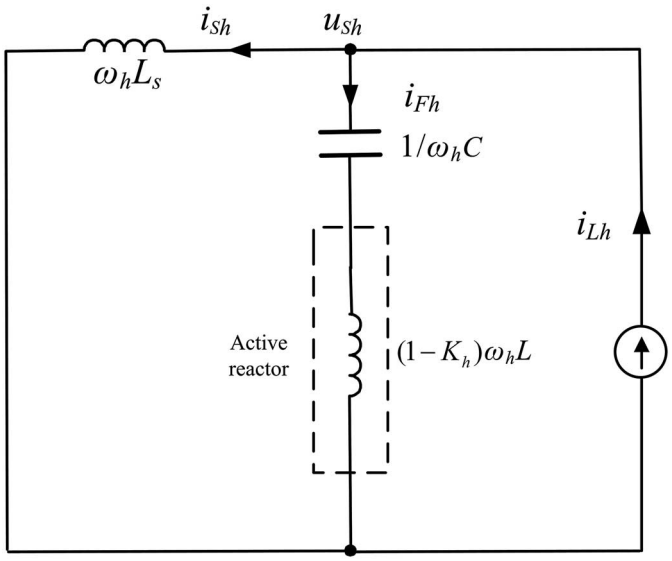

Fig. 3. Principle analysis of ATHPF.

harmonic content of the voltage across the filter reactor and capacitor, respectively.

Suppose that the h-order harmonic current injected into ATHPF is expressed as follows:

$$i_{Fh} = I_{Fh} \sin(\omega_h t + \varphi_h) \tag{2}$$

where φ_h is the phase angle relative to the source voltage.

The APF is controlled as a current source and its output current $i_{\text{APF}.h}$ satisfies the following relationship:

$$i_{\text{APF}.h} = K_h \cdot i_{Fh} \tag{3}$$

where K_h is the control gain for h-order harmonic.

Then solve (1)–(3), and the u_{Sh} can be derived as

$$u_{Sh} = \frac{(1-K_h)\omega_h^2 LC - 1}{\omega_h C} I_{Fh} \cos(\omega_h t + \varphi_h). \tag{4}$$

This indicates that the external impedance seen from the installation point of ATHPF at h-order harmonic frequency can be written as

$$Z_{\text{ATHPF}.h} = (1-K_h)\,\omega_h L - \frac{1}{\omega_h C}. \tag{5}$$

In fact, we can further obtain the h-order harmonic equivalent inductance $L_{\text{eq}.h}$

$$L_{eq.h} = (1-K_h)\,L. \tag{6}$$

The above formula shows that the aggregate of APF and the reactor L can be regarded as a controllable active reactor. The equivalent inductance at the h-order harmonic frequency can be adjusted continuously by regulating the amplitude and sign of the gain K_h. In other words, if K_h increases, the equivalent inductance at h-order harmonic frequency will decrease, and vice versa. Therefore, the single-phase circuit in Fig. 2 is equivalent to that in Fig. 3.

Referring to Fig. 3, the attenuation factors I_{Sh}/I_{Lh} and I_{Fh}/I_{Lh} are expressed as follows:

$$\frac{I_{Sh}}{I_{Lh}} = \frac{(1-K_h)\omega_h L - 1/\omega_h C}{\omega_h L_S + (1-K_h)\omega_h L - 1/\omega_h C} \tag{7}$$

$$\frac{I_{Fh}}{I_{Lh}} = \frac{\omega_h L_S}{\omega_h L_S + (1-K_h)\omega_h L - 1/\omega_h C}. \tag{8}$$

If K_h meets the following formula:

$$(1-K_h)\omega_h L - \frac{1}{\omega_h C} = 0 \tag{9}$$

then

$$I_{Sh} = 0$$

$$I_{Fh} = I_{Lh}.$$

Referring to (9), K_h can be deduced as follows:

$$K_h = \begin{cases} 1 - \frac{1}{\omega_h^2 LC}, & h \in G \\ 0, & h \notin G \end{cases} \tag{10}$$

where G is the set of selective harmonic orders to be suppressed. For example, if the ATHPF is intended to eliminate 5, 7, 11, 13, and 17 orders harmonic currents, the set G can be expressed as $G = \{5, 7, 11, 13, 17\}$.

Let ω_r be the designed resonant angular frequency of the *LC* filter. That is,

$$1 - \omega_r^2 LC = 0. \tag{11}$$

Applying (11) into (10), we can further obtain the expression of K_h

$$K_h = \begin{cases} 1 - \frac{1}{\omega_h^2 LC} = 1 - \left(\frac{\omega_r}{\omega_h}\right)^2, & h \in G \\ 0, & h \notin G. \end{cases} \tag{12}$$

When K_h satisfies (12), no h-order harmonic current appears in the power system. At the same time, the h-order harmonic current flowing into ATHPF reaches the maximum value which equals to the h-order harmonic current in the nonlinear load. This is referred to as normal active tuning function and the corresponding implementation method is called the active tuning control principle.

When the denominator of (8) approaches zero, the resonance between the system impedance and the ATHPF occurs. Consequently, a large amount of h-order harmonic current will flow into ATHPF, resulting in damage to the ATHPF. Still, the harmonic current of neighboring nonlinear loads in practical industrial power system will also flow into the filter when ATHPF is well tuned with the active tuning control principle, thus leading to the damage of the ATHPF as well.

According to (8), once the h-order harmonic over-current occurs, the gain K_h is controlled to decrease gradually, resulting in the increase of the equivalent impedance at the h-order harmonic frequency. Hence, the ATHPF deviates from tuning condition to detuning condition preventing the ATHPF from absorbing the h-order harmonic current until the h-order

harmonic current flowing into ATHPF decreases to the permissible value of filter harmonic current. This is referred to as abnormal active detuning function to improve the safety operation of ATHPF without losing harmonic elimination and reactive power compensation at the occurrence of harmonic over-current. The corresponding realization method is called active detuning control principle.

Results of the above analysis indicate that both the normal active tuning function and the abnormal active detuning function can be implemented by adjusting the control gain K_h, namely the APF output current. Based on this concept, a bidirectional control principle for ATHPF is proposed to selectively eliminate harmonic currents and flexibly protect against harmonic over-current simultaneously. The compensation performance and complete implementation method of the bidirectional control principle will be elaborated in Sections III and IV, respectively.

C. System Parameters Selection

In ATHPF, it is important to select the parameters of the *LC* filter, especially the initial inductance L. C is chosen according to the principle presented in [26].

In terms of each harmonic, they share the common capacitor with the same capacitance. For this reason, the filter inductance in ATHPF should have different values at different selective suppressed harmonic frequencies to eliminate the predetermined harmonic currents. The filter inductance at h-order harmonic frequency L_h should be

$$L_h = \frac{1}{\omega_h^2 C} = \frac{1}{h^2 \omega_1^2 C} \tag{13}$$

where ω_1 is the fundamental angular frequency of the power system.

It can be seen from (13) that the required inductance decreases with the increasing harmonic order. If $h_{\min}$ is the minimum harmonic order to be eliminated, the active reactor reaches the maximum inductance at the $h_{\min}$-order harmonic frequency. It is quite risky to select the initial filter inductance L less than the inductance at the $h_{\min}$-order harmonic frequency because it will result in harmonic amplification and harmonic over-current when APF exits from ATHPF due to faults. Therefore, the value of L should be designed as (14) to ensure the filter continuously working in a traditional PPF way when the APF is out of operation

$$L = \frac{1.1}{\omega_{h\,\min}^2 C} = \frac{1.1}{h_{\min}^2 \omega_1^2 C}. \tag{14}$$

III. Compensation Performance Analysis of the Bidirectional Control Principle

Fig. 4 illustrates the APF reference current generation framework with the bidirectional control principle.

The bidirectional control principle for multiple harmonic elimination adopts a parallel operation approach. The generation method for the reference current of each order follows the same procedure. First, the single-order harmonic content is extracted from the filter current. Second, multiplying the obtained harmonic component by $K_h(s)$ gets the corresponding h-order reference current. Finally, the total APF reference current $I_{\text{APF}}(s)$ is produced by adding up the reference current of each order.

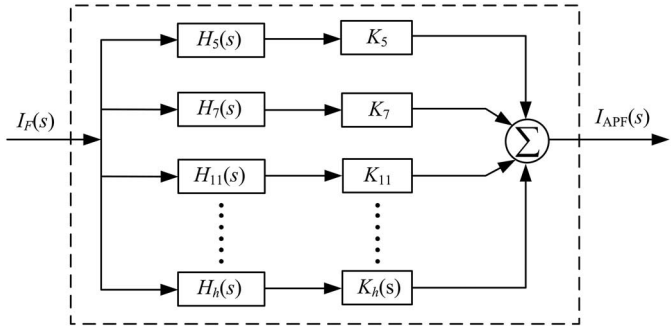

Fig. 4. APF reference current generation.

According to Fig. 4, if the $H_h(s)$ and $H(s)$, respectively, denote the transfer function of single harmonic extraction and the transfer function from $I_F(s)$ to $I_{\text{APF}}(s)$, we can obtain the following formulas:

$$I_{\text{APF}}(s) = H(s) I_F(s) \tag{15}$$

$$H(s) = \sum_{h \in G} K_h(s) H_h(s) \tag{16}$$

$$H_h(s) = \frac{Bs}{s^2 + Bs + \omega_{\text{o}}^2} \tag{17}$$

where B and ω_{o} are band-pass width and central angular frequency, respectively.

The ideal characteristic of $H(s)$ and $H_h(s)$ in terms of h-order harmonic should be

$$H_h(j\omega_o) = \begin{cases} 1, & \omega_o = h\omega_1 \\ 0, & \omega_o \neq h\omega_1 \end{cases} \tag{18}$$

$$H(j\omega_o) = \begin{cases} K_h, & \omega_o = h\omega_1 \ \forall h \in G \\ 0, & \text{otherwise.} \end{cases} \tag{19}$$

Hence, $I_S(s)/I_L(s)$ and $I_F(s)/I_L(s)$ are expressed as follows:

$$\begin{aligned} \frac{I_S(s)}{I_L(s)} &= \frac{1/sC + (1 - H(s))sL}{sL_s + 1/sC + (1 - H(s))sL} \\ &= \frac{1/sC + (1 - \sum_{h \in G} K_h(s) H_h(s))sL}{sL_s + 1/sC + (1 - \sum_{h \in G} K_h(s) H_h(s))sL} \end{aligned} \tag{20}$$

$$\begin{aligned} \frac{I_F(s)}{I_L(s)} &= \frac{sL_s}{sL_s + 1/sC + (1 - H(s))sL} \\ &= \frac{sL_s}{sL_s + 1/sC + (1 - \sum_{h \in G} K_h(s) H_h(s))sL}. \end{aligned} \tag{21}$$

Formulas (20) and (21) can be employed to analyze the compensation performance of the bidirectional control principle including both the active tuning control principle and the active detuning control principle.

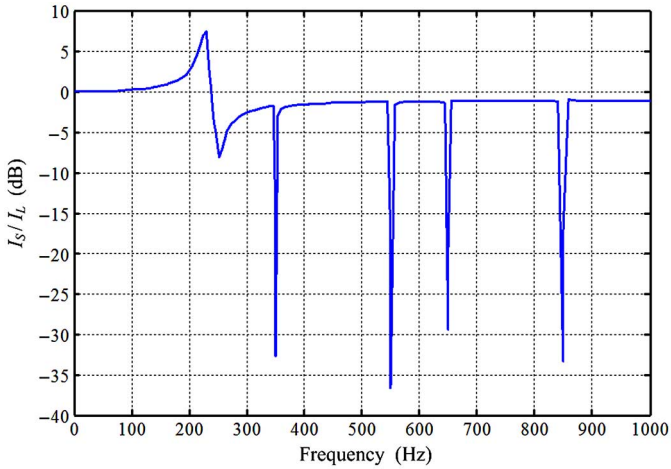

Fig. 5. Bode diagram of $I_S(\mathrm{s})/I_L(\mathrm{s})$.

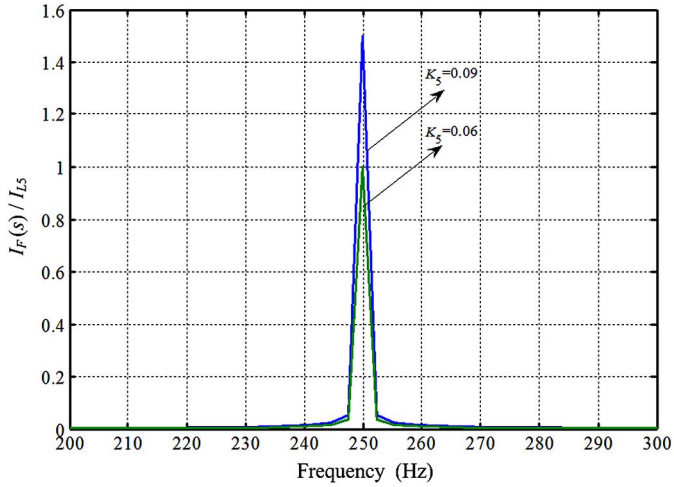

Fig. 6. Magnitude-frequency characteristic of $I_F(\mathrm{s})/I_{L5}$ with different K_5 under over-current of the fifth harmonic.

A. Filtering Performance

Fig. 5 illustrates bode diagram of (20) when the ATHPF is actively tuned at 5, 7, 11, 13, and 17 harmonic frequencies. The *LC* filter resonates at 4.77th harmonic frequency. According to (12), the values of K_h in (20) for 5, 7, 11, 13, and 17 harmonics are 0.09, 0.54, 0.81, 0.87, and 0.92, respectively.

As shown in Fig. 5, we can observe that the amplitudes of $I_S(s)/I_L(s)$ at 5, 7, 11, 13, and 17 harmonic frequencies are significantly attenuated, whereas the magnitudes have no change at other nonselected harmonic frequencies. This indicates that the ATHPF with the active tuning control principle can automatically eliminate the predetermined multiple harmonic currents. The advantage of ATHPF with the active tuning control principle lies in the fact that the filter system only consists of a single *LC* series branch, but it can simultaneously resonate at multiple harmonics without detuning, thus eliminating several selective harmonics.

B. Characteristic of Flexible Protection Against Harmonic Over-Current

When the ATHPF is well tuned at fifth harmonic frequency (250 Hz) with the active tuning control principle, the whole fifth harmonic current I_{L5} in the nonlinear load flows into the ATHPF. At this point, the fifth harmonic over-current easily occurs. If the fifth harmonic current in nonlinear load becomes to 1.5 I_{L5} due to additional fifth harmonic current caused by neighboring uncompensated nonlinear load, the filter current $I_F(s)$ at fifth harmonic frequency is also increased to 1.5 I_{L5}, thus leading to the fifth harmonic over-current of ATHPF. As illustrated in Fig. 6, the ration $I_F(s)/I_L5$ becomes 1.5 at the fifth harmonic frequency at this time. Nevertheless, the filter current $I_F(s)$ at fifth harmonic frequency can be reduced to the permissible value I_{L5} with K_5 decreased from 0.09 to 0.06. As illustrated in Fig. 6, the ration $I_F(s)/I_{L5}$ at the fifth harmonic frequency is reduced to 1 with decreased K_5.

The analysis result proves that the h-order harmonic current flowing into ATHPF can be effectively prevented by adjusting the corresponding h-order harmonic control gain K_h, thus protecting the ATHPF against harmonic over-current.

IV. Realization of the Bidirectional Control Principle

A. Adjusting Method for K_h

Results of analysis in Section III indicate that the bidirectional control principle with both the normal active tuning function and the abnormal active detuning function can be implemented by adjusting the control gain K_h.

In order to realize the normal active tuning function, the theoretical value of K_h can be obtained according to (12). However, there are deviations of system frequency and the *LC* parameters in engineering application. Hence, if the calculated K_h in terms of (12) is still chosen as the control basis, the satisfactory filtering performance cannot be achieved sometimes. Therefore, K_h should be adjusted continuously according to the practical operation condition of ATHPF. In addition, when ATHPF implements the abnormal active detuning function, K_h should also be regulated constantly according to the practical harmonic current flowing into ATHPF and the designed permissible value of filter harmonic current.

Because both the normal active tuning function and abnormal active detuning function are implemented by regulating the filter detuning, the degree of filter detuning is chosen as the control basis for ATHPF. Fig. 7 shows a schematic diagram of the bidirectional control principle with the K_h adjusting. For the h-order harmonic, the difference between the practical detuning δ and its reference δ^* is obtained at first, and K_h is then obtained by means of proportional integral (PI) regulator. After that, by means of multiplying the obtained gain K_h by h-order harmonic component of the current flowing into ATHPF, the h-order reference current $i_{\mathrm{APF}.h}$ is generated. Finally, the reference current $i_{\mathrm{APF}.h}$ is sent to pulse-width modulation (PWM) generator and driver to produce the driving signals of the switching devices.

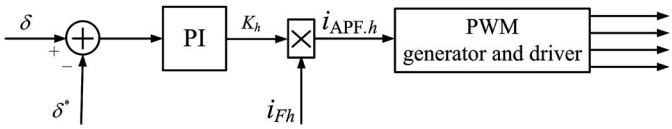

Fig. 7. Schematic diagram of the bidirectional control.

One of the key links in Fig. 7 is the online detection method for the practical detuning δ of the h-order harmonic. Formula (22) is employed to obtain δ indirectly in this paper

$$\delta = \frac{U_{Lh} - U_{Ch}}{U_{Lh} + U_{Ch}} \tag{22}$$

where U_{Lh} and U_{Ch} are root-mean-square (rms) values of the h-order harmonic content of the voltage across the filter reactor and capacitor, respectively.

The following analysis proves that the measured detuning δ according to (22) shows good performance to indicate the theoretical detuning δ_0.

Suppose that X_{Lh} and X_{Ch} are the h-order harmonic impedances of the filter reactor and capacitor, respectively. According to (22), δ can be further expressed as (23) under the assumption that the inherent resistor of the filter reactor is zero. This indicates that the quality factor of filter reactor tends to be infinite in (23)

$$\delta = \frac{U_{Lh} - U_{Ch}}{U_{Lh} + U_{Ch}} = \frac{X_{Lh} - X_{Ch}}{X_{Lh} + X_{Ch}} = \frac{\omega_h^2 LC - 1}{\omega_h^2 LC + 1}. \tag{23}$$

According to the filter detuning definition, the h-order theoretical detuning δ_0 can be expressed as follows:

$$\delta_0 = \frac{\omega_h - \omega_r}{\omega_h}. \tag{24}$$

Then applying (11) and (24) into (23), we can further obtain the relationship between the measured detuning δ and the theoretical detuning δ_0

$$\delta = \frac{1 - (1 - \delta_0)^2}{1 + (1 - \delta_0)^2}. \tag{25}$$

Fig. 8 illustrates the relationship between the theoretical detuning δ_0 and the measured detuning δ according to (25) on the closed interval $[-0.2, 0.2]$. It can be seen from Fig. 8 that there is a satisfactory linear relationship between δ and δ_0 in the range of $-0.2 \le \delta_0 \le 0.2$.

In fact, the following formula can be established considering that the filter detuning usually varies on the closed interval $[-0.2, 0.2]$

$$\delta = \frac{1 - (1 - \delta_0)^2}{1 + (1 - \delta_0)^2} = \frac{2\delta_0 - \delta_0^2}{2 + \delta_0^2 - 2\delta_0} = \frac{2\delta_0}{2 - 2\delta_0} \approx \delta_0. \tag{26}$$

Combining Fig. 8 with (26), we can observe that the practical detuning of the h-order harmonic can be obtained indirectly by means of detecting the h-order harmonic component of the voltage across the filter reactor and the capacitor of the *LC* filter, respectively.

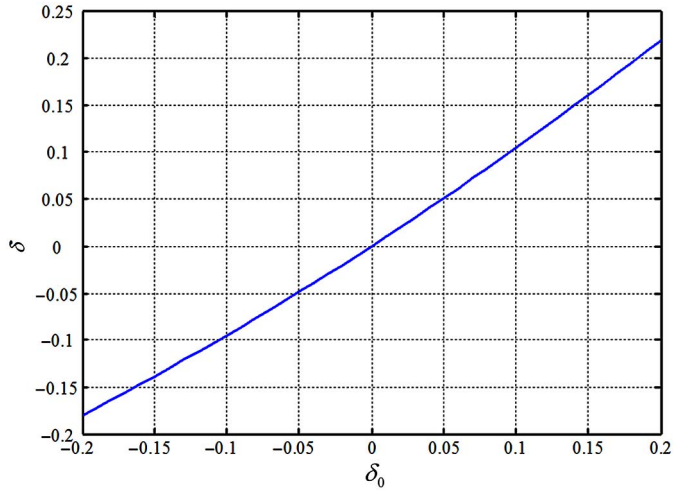

Fig. 8. Relationship between δ and δ_0.

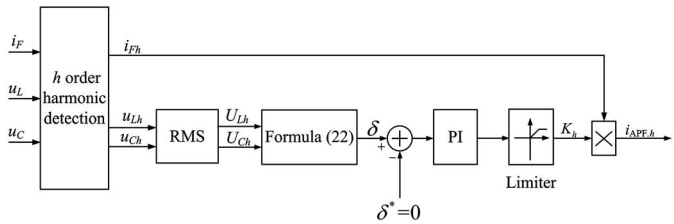

Fig. 9. Active tuning realization of the h-order harmonic.

B. Control Scheme to Realize the Normal Active Tuning Function

Fig. 9 demonstrates how the control scheme realizes the normal active tuning function for ATHPF. For h-order harmonic, the control objective of the normal active tuning function is to make ATHPF well resonate at h-order harmonic frequency. Consequently, the reference detuning δ^* is set as zero under this operating condition.

The specific implementing procedure of the control scheme presented in Fig. 9 is described as follows. Based on the single-order harmonic detection method such as fast Fourier transform, the h-order harmonic components i_{Fh}, u_{Lh}, and u_{Ch} are successively extracted from the filter current, the voltage across the filter reactor, and the capacitor. In addition, the corresponding rms values U_{Lh} and U_{Ch} are also calculated. After that, the h-order practical detuning δ is obtained according to (22). Finally, the PI regulator adjusts the control gain K_h in such a way so as to make δ equal to δ^* (δ^* equals to 0 in this case). As a result, the ATHPF can automatically resonate at the h-order harmonic frequency without detuning.

C. Control Scheme to Realize the Abnormal Active Detuning Function

The h-order harmonic over-current easily occurs when ATHPF is well tuned at h-order harmonic frequency with the control scheme presented in Fig. 9. Once the actual harmonic current flowing into ATHPF is larger than the designed permissible value of filter harmonic current, the harmonic over-current phenomenon occurs. In order to reduce the h-order harmonic

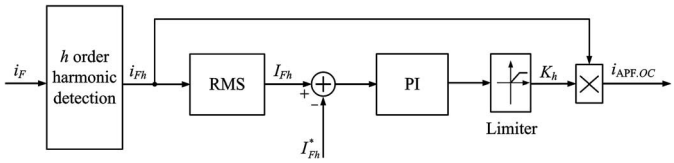

Fig. 10. Active detuning realization under over-current of the h-order harmonic.

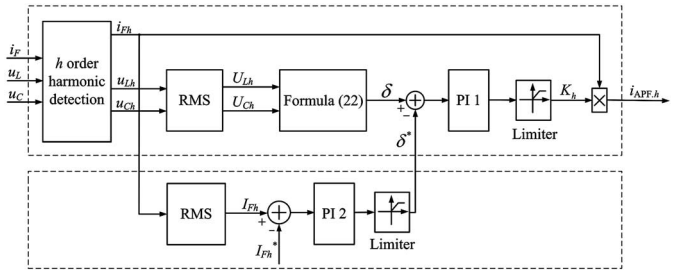

Fig. 11. Bidirectional control realization of the h-order harmonic.

current flowing into ATHPF to the designed permissible value, a flexible protection is adopted to make the ATHPF deviate from tuning point by adjusting K_h and APF output current.

As far as h-order harmonic is concerned, Fig. 10 shows how the control scheme realizes the abnormal active detuning function. To begin with, the h-order harmonic component i_{Fh} is extracted from the filter current, and the corresponding rms values I_{Fh} are also calculated. Next, the limitation I^*_{Fh} is designed according to the permissible value of harmonic current flowing into the filter. The permissible value should be precalculated according to filter designed capacity of h-order harmonic over-current. After that, the gain K_h is produced by PI regulator according to the difference between I_{Fh} and I^*_{Fh}. To be specific, when I_{Fh} is smaller than I^*_{Fh}, the gain K_h is set as zero. Once I_{Fh} is larger than I^*_{Fh}, the PI regulator adjusts the gain K_h so as to make I_{Fh} equal to I^*_{Fh}. Finally, the reference current $i_{\text{APF.OC}}$ is generated through multiplying K_h by i_{Fh}.

The advantage of this protection method lies in the fact that the filter system does not have to be switched-OFF from the power system at the occurrence of harmonic over-current, thus realizing the flexible protection against the h-order harmonic over-current to ensure the safe operation of ATHPF without losing harmonic elimination and reactive power compensation.

D. Control Scheme to Realize the Bidirectional Control Principle

In terms of h-order harmonic, Fig. 11 illustrates how the control scheme realizes the bidirectional control principle, which combines the control scheme presented in Fig. 9 with the control scheme presented in Fig. 10. In Fig. 11, the generation method of practical detuning δ is similar to that in Fig. 9. In the following, the method to obtain the reference detuning δ^* in the bidirectional control principle of the h-order harmonic is elaborated.

As illustrated in Fig. 11, when the h-order harmonic over-current does not occur, i.e., when the h-order practical current

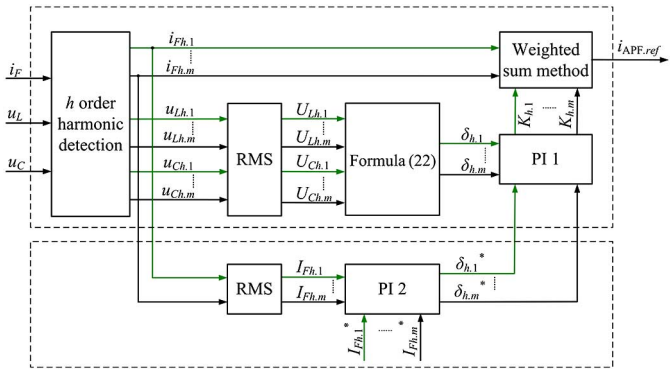

Fig. 12. Bidirectional control realization of multiple selective harmonics.

flowing into ATHPF I_{Fh} is smaller than its reference I^*_{Fh}, δ^* is set as zero in order to achieve the h-order harmonic elimination performance. Once the h-order harmonic over-current occurs, i.e., I_{Fh} is larger than I^*_{Fh}, δ^* is gradually increased through PI regulator 2 so as to make ATHPF deviate actively from the tuning condition to the detuning condition. This process lasts until I_{Fh} equals to I^*_{Fh}. After both the practical detuning δ and its reference δ^* are obtained, the control gain K_h can be produced by PI regulator 1 according to the error between δ and δ^*. Finally, the reference current of the h-order harmonic $i_{\text{APF}.h}$ is generated through multiplying the K_h by the h-order harmonic content of filter current.

E. Control Scheme to Realize the Bidirectional Control Principle for Multiple Selective Harmonics

Fig. 12 illustrates how the control scheme realizes the bidirectional control principle for multiple selective harmonics. The reference current for each order harmonic follows the same procedure presented in Fig. 11. The total harmonic reference current $i_{\text{APF.ref}}$ is achieved by adding up the reference current of each order.

To begin with, for the harmonic currents intended to be eliminated in the power system, each harmonic component $i_{Fh.1}$ to $i_{Fh.m}$ is extracted from i_F and the rms values $I_{Fh.1}$ to $I_{Fh.m}$ are also calculated. Meanwhile, the reference detunings $\delta^*_{h.1}$ to $\delta^*_{h.m}$ are produced through PI regulator 2 according to the corresponding errors between the practical values $I_{Fh.1}$ to $I_{Fh.m}$ and the precalculated references $I^*_{Fh.1}$ to $I^*_{Fh.m}$. Then, each rms values of the harmonic voltage across the filter reactor and capacitor $U_{Lh.1}$ to $U_{Lh.m}$ and $U_{Ch.1}$ to $U_{Ch.m}$ are calculated through single-order harmonic extraction and rms calculation, respectively. Furthermore, the practical detunings $\delta_{h.1}$ to $\delta_{h.m}$ are calculated according to (22). After both the practical detunings and the references are obtained, we can get the control gains $K_{h.1}$ to $K_{h.m}$ by means of PI regulator 1 according to the corresponding differences between $\delta_{h.1}$ to $\delta_{h.m}$ and $\delta^*_{h.1}$ to $\delta^*_{h.m}$. Finally, the total APF reference current is determined through multiplying $i_{Fh.1}$ to $i_{Fh.m}$ by $K_{h.1}$ to $K_{h.m}$ with weighted sum method. Moreover, the bidirectional control principle of ATHPF compensating fifth and seventh harmonics is given as an example to elaborate the APF total reference generation method using weighted sum method.

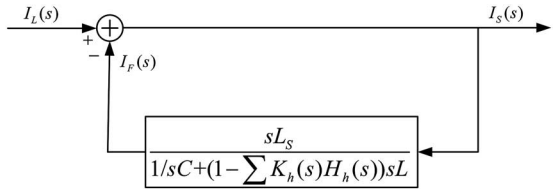

Fig. 13. Control block diagram of ATHPF with active tuning control.

First, multiplying the fifth control gain K_5 by the fifth harmonic current flowing into the filter i_{F5} can produce the fifth reference current $i_{\text{APF.5}}$. Secondly, multiplying the seventh control gain K_7 by the seventh harmonic current flowing into the filter i_{F7} can generate the seventh reference current $i_{APF.7}$. Finally, the total reference current for the fifth and seventh harmonic elimination $i_{\text{APF.ref}}$ is determined by adding up $i_{\text{APF.5}}$ and $i_{\text{APF.7}}$.

V. Parameters Selection for Control

A. Parameters Selection for Active Tuning Control

Fig. 13 shows the control block diagram of ATHPF, where $I_L(s)$, $I_F(s)$, and $I_S(s)$ are considered as the input signal, feedback signal, and error signal, respectively. Therefore, formula (20) can be regarded as the transfer function of the active tuning control principle.

According to the active tuning control principle presented in Fig. 11, we can obtain

$$K_h(s) = \frac{U_{Lh} - U_{Ch}}{U_{Lh} + U_{Ch}} G_{PI1}(s) \tag{27}$$

$$G_{PI1}(s) = K_{P1}\left(1 + \frac{1}{T_{i1}s}\right) \tag{28}$$

where K_{P1} and T_{i1} are proportional coefficient and integration time constant for PI 1 in Fig. 11.

Applying (6) and (22) into (27), we can obtain the following relationship:

$$K_h(s) = \frac{\omega_h^2 L(1 - K_h(s))C - 1}{\omega_h^2 L(1 - K_h(s))C + 1} G_{PI1}(s). \tag{29}$$

Then

$$K_h(s) = \frac{(\omega_h^2 LC - 1)G_{PI1}(s)}{\omega_h^2 LC(1 + G_{PI1}(s)) + 1}. \tag{30}$$

Applying (30) into (20), the characteristic equation of the active tuning control principle with h-order harmonic elimination can be written as

$$e_1 s^5 + e_2 s^4 + e_3 s^3 + e_4 s^2 + e_5 s^1 + e_6 = 0 \tag{31}$$

TABLE I
Routh Table

Polynomial	Coefficient		
S^5	e_1	e_3	e_5
S^4	e_2	e_4	e_6
S^3	d_1	d_2	
S^2	f_1	f_2	
S^1	g_1		
S^0	h_1		

where

$$\begin{aligned}
e_1 &= (L_S + L)CT_{i1} \\
e_2 &= 1/\omega_h^2 C + m_1 K_{P1} \\
e_3 &= Bm_2 ar \\
e_4 &= m_3(L_S + L)K_{P1}T_{i1} + r/\omega_h C \\
e_5 &= 1 + m_1 m_3 L \\
e_6 &= \omega_h^2 L_S
\end{aligned}$$

where

$$\begin{aligned}
a &= K_{P1}T_{i1} \\
m_1 &= (\omega_h^2 LC - 1)/(\omega_h^2 LC + 1) \\
m_2 &= \omega_h L + 1/\omega_h C \\
m_3 &= \omega_h^2 CB \\
r &= 1 - K_{P1}.
\end{aligned}$$

Then the Routh table can be obtained as shown in Table I. In which,

$$\begin{aligned}
d_1 &= \frac{e_2 e_3 - e_1 e_4}{e_2}, \\
d_2 &= \frac{e_2 e_5 - e_1 e_6}{e_2}, \\
f_1 &= \frac{d_1 e_4 - d_2 e_2}{d_1}, \\
f_2 &= e_6, \\
g_1 &= \frac{f_1 d_2 - f_2 d_1}{f_1}, \\
h_1 &= f_2.
\end{aligned}$$

Using the Routh criterion, we can get the stability condition of ATHPF with the active tuning control principle is

$$\begin{cases} e_2 e_3 - e_1 e_4 > 0 \\ d_1 e_4 - d_2 e_2 > 0 \\ f_1 d_2 - f_2 d_1 > 0. \end{cases} \tag{32}$$

Solve (32) with system parameters in Table II, and the stable region for fifth harmonic elimination is shown in Fig. 14.

TABLE II
PARAMETERS OF ATHPF

Variable	Value	Description
U_S	220 V	Rated voltage
SCC	20 kVA	Short-circuit capacity
f_S	50 Hz	Frequency of system
R_{Load}	15 Ω	Load resistance of the diode rectifier
L_{Load}	100 mH	Load inductance of the diode rectifier
C	75 μF	Filter capacitance
L	17 mH	Filter inductance
Q_{filter}	1140 VA	Rating of LC filter
q	30	Quality factor of LC filter
f_s	9600 Hz	Switching frequency of APF
Q_{APF}	42 VA	Rating of APF

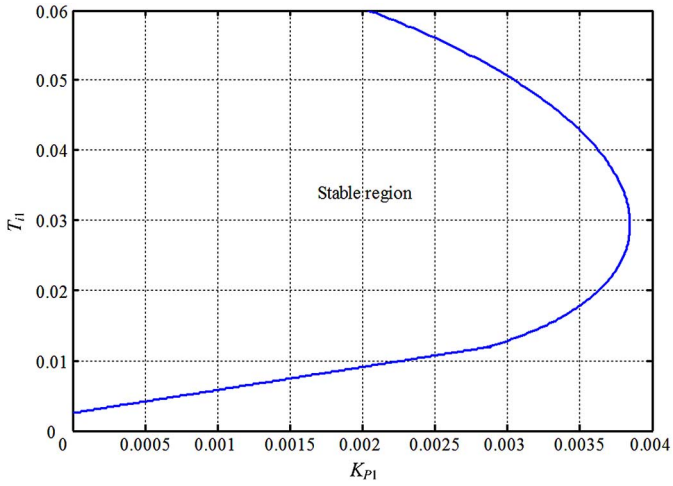

Fig. 14. Parameters selection for active tuning control.

For active tuning control of ATHPF, the open-loop transfer function $G_{\text{ol.1}}(\text{s})$ with system parameters in Table II for fifth harmonic elimination is given by (33), which is shown at the bottom of the page.

In considering the range of K_{P1} and T_{i1} illustrated in Fig. 14, $0.005T_{i1}s^4$ and $(0.005 + 0.51K_{P1})s^3$ can be ignored and then the approximate expression of (33) is written as

$$G_{\text{ol.1}}(s) = \frac{1275(0.116\,s + 1)}{s(8.6(1 - K_{P1})s + 1)(392.5K_{P1}T_{i1}s + 1)}. \tag{34}$$

Due to the fact that $8.6(1 - K_{P1})$ is much larger than $392.5K_{P1}T_{i1}$, then (34) is further simplified as

$$G_{\text{ol.1}}(s) = \frac{1275}{8.6(1 - K_{P1})} \cdot \frac{(0.116\,s + 1)}{s^2(392.5K_{P1}T_{i1}s + 1)}. \tag{35}$$

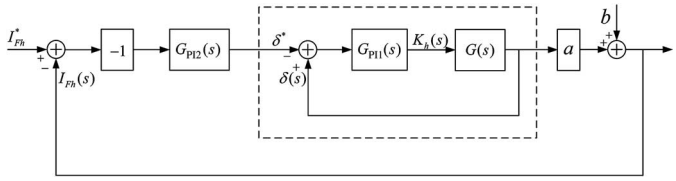

Fig. 15. Control block diagram of ATHPF with active detuning control.

According to the design criteria of third-order optimum system, the following formulas are established:

$$\begin{cases} 1275/8.6(1 - K_{P1}) = 1/(8 \times (392.5K_{P1}T_{i1})^2) \\ 4 \times 392.5K_{P1}T_{i1} = 0.116. \end{cases} \tag{36}$$

Finally, K_{P1} and T_{i1} are derived as

$$\begin{cases} K_{P1} = 0.0025 \\ T_{i1} = 0.03. \end{cases} \tag{37}$$

B. Parameters Selection for Active Detuning Control

According to the definition of quality factor, the following formula is obtained:

$$q = \frac{\omega_r L}{R} \tag{38}$$

where q and R are quality factor and equivalent resistance of the tuned filter, respectively.

Combining (24) with (38), we can get

$$X_{Lh} - X_{Ch} = \omega_h L - \frac{1}{\omega_h C} = \frac{\omega_r L}{1 - \delta} - \frac{1 - \delta}{\omega_r C} \approx 2qR\delta.$$

From the equivalent circuit shown in Fig. 3, the relationship between $I_{Fh}(s)$ and $\delta(s)$ can be expressed as

$$I_{Fh}(s) = \frac{\omega_h L_S}{\omega_h L_S + 2qR\delta(s)} I_{Lh}. \tag{39}$$

Moreover, (39) can be fitted as the following linear equation by curve fitting method. That is,

$$I_{Fh}(s) = a\delta(s) + b \tag{40}$$

where a and b are fitting coefficients.

For fifth harmonic, we can obtain that a and b are -1.45 and 0.81 by fitting (39) with system parameters in Table II.

Then the control block diagram of ATHPF with active detuning control principle is illustrated in Fig. 15.

In Fig. 15, the dashed frame is the inner loop for active tuning control, and the closed-loop transfer function of inner loop

$$G_{\text{ol.1}}(s) = \frac{1275(0.116\,s + 1)}{s(0.005T_{i1}s^4 + (0.005 + 0.51K_{P1})s^3 + 3375(1 - K_{P1})K_{P1}T_{i1}s^2 + (392.5K_{P1}T_{i1} - 8.6K_{P1} + 8.6)s + 1)}. \tag{33}$$

$G_{\text{inner}}(s)$ can be regarded as a first-order inertia element after regulating. That is,

$$G_{\text{inner}}(s) = \frac{G_{PI1}(s)G(s)}{G_{PI1}(s)G(s)-1} = \frac{1}{\tau s+1}$$

where the time constant τ is usually several times of PWM switching period and τ is designed as $0.001s$ in this example.

The expression of $G_{PI2}(s)$ in Fig. 15 is

$$G_{PI2}(s) = K_{P2}\left(1+\frac{1}{T_{i2}s}\right)$$

where K_{P2} and T_{i2} are proportional coefficient and integration time constant for PI 2 in Fig. 11.

Then the open-loop transfer function $G_{\text{ol}.2}(s)$ with system parameters in Table II is

$$G_{\text{ol}.2}(s) = \frac{1.45K_{P2}}{T_{i2}}\frac{(T_{i2}s+1)}{s(0.001\,s+1)}.$$

T_{i2} can be selected as

$$T_{i2} = 0.001/10 = 0.0001.$$

According to the design criteria of I-type system, the following formula is established

$$\left(\frac{1.45K_{P2}}{T_{i2}}\right)\cdot 0.001 = 0.5.$$

That is,

$$K_{P2} = 0.034.$$

VI. Experimental Results

A laboratory prototype of ATHPF based on the proposed bidirectional control principle has been manufactured to evaluate the performance of selective harmonic elimination and flexible protection against harmonic over-current predicted by the previous theoretical analysis. Fig. 16 shows the hardware implementation of ATHPF with the bidirectional control principle, in which the digital signal controller is adopted as the main processor for digital control of ATHPF. The digital signal controller is used for data sampling, calculating, the bidirectional control principle realization and PWM generating. Table II summarizes the parameters of ATHPF.

A. Experiment of Harmonic Elimination

Fig. 17(a)–(f), respectively, illustrates the source current waveforms and spectrums in the following three cases.

1) No power filter is connected.
2) Only the *LC* filter is connected.
3) Both the *LC* filter and the APF are connected.

Moreover, Table III summarizes the test results of main harmonic percentage in the source current with the help of power analyzer HIOKI3166. In Table III, the fundamental current of the nonlinear load current (8 A) is chosen as the base value of current. The waveforms are recorded by the digital oscilloscope DPO3034.

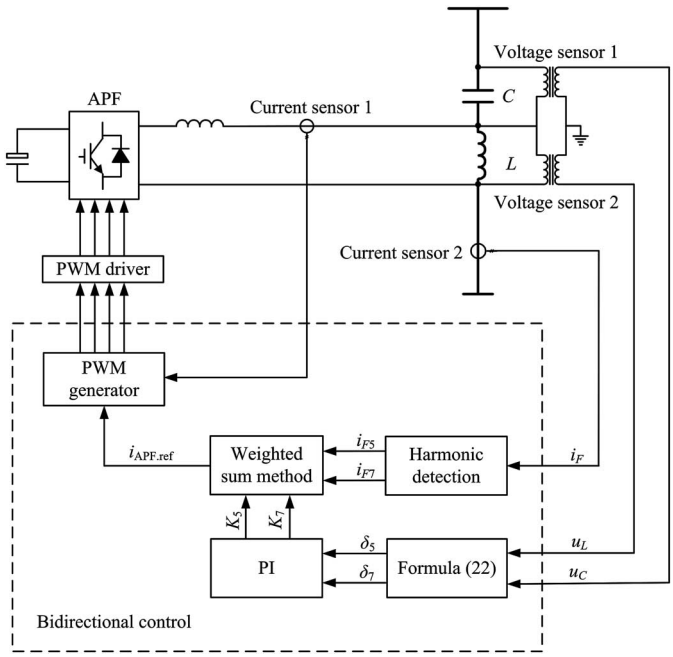

Fig. 16. Hardware implementation of ATHPF.

From Fig. 17(a) and (b), it can be observed that the total harmonic distortion (THD) of the source current reaches 25.5% when no filter is connected. The source current waveform is approximately a square wave with rich harmonics. Apparently, serious distortion exists in the source current, and the third, fifth, and seventh harmonic currents in the power system reach 20.0%, 11.6%, and 7.6%, respectively, as presented in Table III.

From Fig. 17(c) and (d), it can be seen that the THD of the source current is reduced to 8.9% when only the *LC* filter is added. The third harmonic current is reduced considerably. From Table III, we can obtain that the third, fifth, and seventh harmonic currents are reduced to 3.0%, 7.9%, and 5.6%, respectively.

From Fig. 17(e) and (f), it can be seen that the THD of the source current further decreases to 4.8% when APF is added, indicating that the whole ATHPF system works. The source current waveform approaches to a sinusoidal wave with the third, fifth, and seventh harmonic currents decreased to 3.0%, 1.6%, and 1.3%, respectively. This indicates that the proposed bidirectional control principle exhibits excellent performance in eliminating multiple selective harmonic currents.

It is noteworthy that the third harmonic current caused by the nonlinear load is mainly suppressed with the help of the *LC* filter whose resonant frequency is around the third harmonic frequency. The fifth and seventh harmonic currents are mainly suppressed by ATHPF with the bidirectional control principle.

In addition, it can be seen that the fundamental component of the source current with the *LC* filter connected becomes larger compared to that without any filter added. This phenomenon is caused by reactive power produced by the *LC* filter. In fact, the power factor of the diode rectifier with resistance–inductance load is high and only little reactive power exists in the nonlinear load. Therefore, the reactive current caused by the *LC* filter

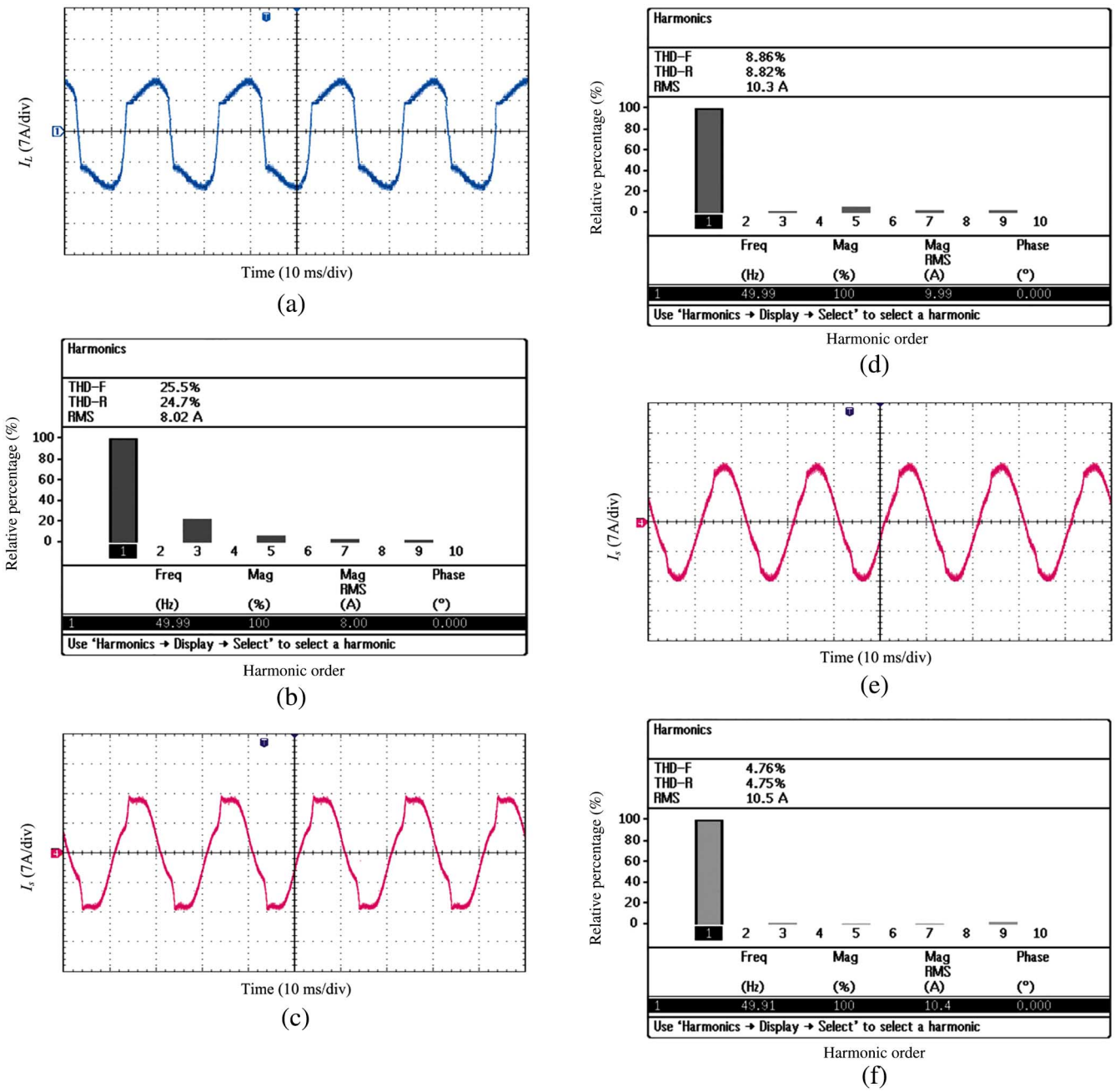

Fig. 17. Filtering performance of ATHPF with active tuning control. Waveform (a) source current without filter added. Waveform (b) Spectrum of source current without filter added. Waveform (c) Source current with only the *LC* filter added. Waveform (d) Spectrum of source current with only the *LC* filter added. Waveform (e) Source current with the whole filter added. Waveform (f) Spectrum of source current with the whole filter added.

flows into the power system, leading to the increase in fundamental component in the source current when the *LC* filter is connected.

B. Experiment of Flexible Protection Against Harmonic Over-Current

In the test system of flexible protection against harmonic over-current, the harmonic over-current phenomenon is simulated by switching ON/OFF the load resistance of the diode rectifier. When the load resistance is switched to 30 Ω, the rms values of nonlinear load current and source current with ATHPF working are 4 and 7 A, respectively. Besides, when the load resistance is switched to 15 Ω, the rms values of nonlinear load current and source current with ATHPF working are increased to 8 and 10 A, respectively.

Figs. 18 and 19 illustrate the waveforms in the following two cases. One is the case in which the harmonic over-current is not considered and the other is the case in which the harmonic over-current is considered. In the former case, the filter detuning references for the fifth and seventh harmonics are always set as zero in the bidirectional principle illustrated in Fig. 12. In the latter case, once the harmonic over-current occurs, the filter detuning references for the fifth and seventh harmonics are

TABLE III
MAIN HARMONIC PERCENTAGE IN SOURCE CURRENT

	Load current	Source current with the *LC* filter	Source current with the whole ATHPF
Fundamental	1	1.25	1.25
3rd (%)	20.0	3.0	3.0
5th (%)	11.6	7.9	1.6
7th (%)	7.6	5.6	1.3
9th (%)	5.6	3.9	3.9
11th (%)	4.0	2.5	2.5
13th (%)	2.9	1.4	1.4
THD (%)	25.5	8.9	4.8

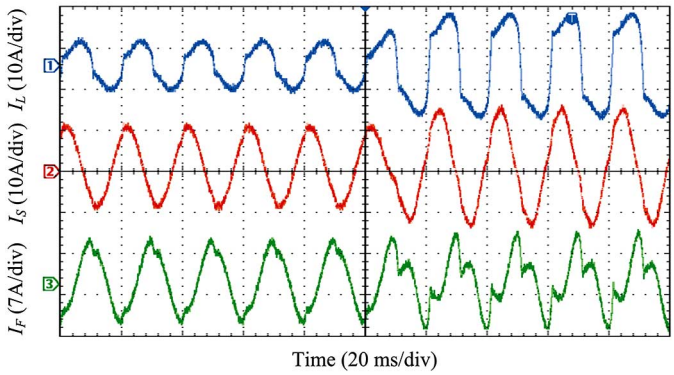

Fig. 18. Current waveforms without harmonic over-current protection when the load resistance is decreased.

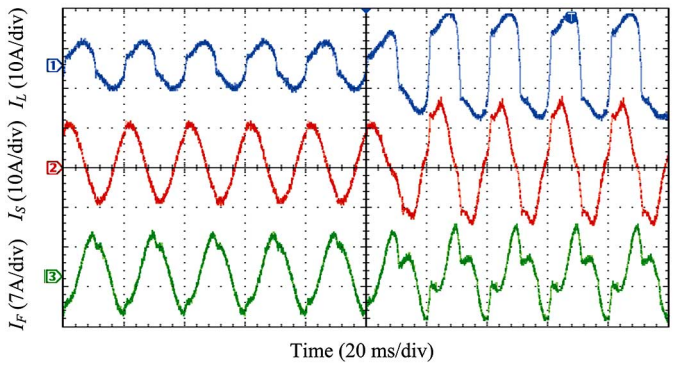

Fig. 19. Current waveforms with harmonic over-current protection when the load resistance is decreased.

continuously adjusting until the fifth and seventh harmonic currents flowing into ATHPF reach the permissible values of the fifth and seventh harmonic currents flowing into the filter.

In Figs. 18 and 19, the waveforms from the top to the bottom are load current, source current with ATHPF added, and filter current, successively. Table IV presents the main harmonic contents of the source current and filter current in Figs. 18 and 19 after the occurrence of harmonic over-current.

In Figs. 18 and 19, when the load resistance of the diode rectifier is 30 Ω, namely before the occurrence of the fifth and seventh harmonics over-current, ATHPF exhibits satisfactory filtering performance. Test results acquired by HIOKI3166 show that the attenuation factors of the source harmonic current I_{S5}/I_{L5} and I_{S7}/I_{L7} are 0.14 and 0.17, respectively.

TABLE IV
COMPARISON BETWEEN ACTIVE TUNING AND BIDIRECTIONAL CONTROL OF MAIN HARMONIC IN THE SOURCE CURRENT

	Lod current (A)	Current with active tuning control		Current with bidirectional control	
		Source current (A)	Filter current (A)	Source current (A)	Filter current (A)
Fundamental	8.0	10.0	5.25	10.0	5.25
3rd	1.60	0.24	1.36	0.24	1.36
5th	0.93	0.13	0.80	0.43	0.50
7th	0.61	0.10	0.51	0.41	0.20
9th	0.45	0.31	0.14	0.31	0.14
11th	0.32	0.20	0.12	0.20	0.12
13th	0.23	0.11	0.12	0.11	0.12
THD (%)	25.5	4.8	31.9	7.5	28.2

The ATHPF succeeds the expected purpose to simultaneously eliminate the fifth and seventh harmonic currents before the occurrence of harmonic over-current.

In Fig. 18, when the load resistance of the diode rectifier is switched from 30 to 15 Ω, the fifth and seventh harmonic currents flowing into ATHPF finally reach to 0.80 and 0.51 A, respectively, as presented in Table IV. It can be seen that the fifth and seventh harmonic currents are over the limitations 0.50 and 0.20 A at this moment, thus causing the fifth and seventh harmonic over-current occurrence.

However, in Fig. 19, when the load resistance of the diode rectifier is switched from 30 to 15 Ω, the filter detuning references for the fifth and seventh harmonics start to increase gradually. As a result, the fifth and seventh harmonic currents in ATHPF eventually decreased to the limitations 0.50 and 0.20 A, as presented in Table IV. This indicates that ATHPF with the bidirectional control principle contributes significantly to the protection against harmonic over-current of ATHPF.

In particular, combining the data in Table IV with the waveforms in Figs. 18 and 19, we can find that the source current in Fig. 19 is becoming worse compared with that in Fig. 18 at the occurrence of harmonic over-current. This is because the additional fifth and seventh harmonic currents flowing into the ATHPF are forced to inject into the power system.

Fig. 20 illustrates the current waveforms when the load resistance of the diode rectifier is switched back from 15 to 30 Ω. The waveforms from the top to the bottom are load current, source current, and filter current, successively. From Fig. 19, we draw such conclusion that the ATHPF employing the bidirectional control principle can return to satisfactory filtering performance after the disappearance of harmonic over-current.

Additionally, from Figs. 18 to 20, it can be observed that the whole regulation process has not only quickly dynamic respond performance but also a nonovershoot characteristic. All the above experimental results have validated the feasibility and effectiveness of the proposed bidirectional control principle in selective harmonic elimination and flexible protection against harmonic over-current.

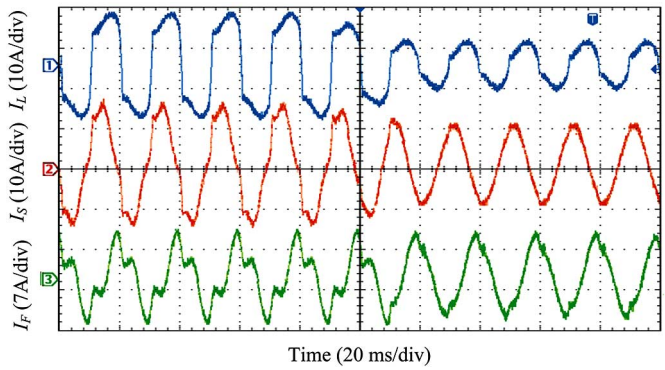

Fig. 20. Current waveforms when the load resistance is increased.

VII. Conclusion

This paper has proposed a bidirectional control principle of ATHPF intended for selective harmonic elimination and flexible protection against harmonic over-current.

Theoretical analysis and experiments developed in this paper have both verified the viability of the proposed bidirectional control principle of ATHPF. Only a single-phase ATHPF based on the bidirectional control principle is discussed in detail in this paper. The realization of three-phase ATHPF could be easily accomplished by employing the same principle.

This paper has mainly led to the following conclusions.

1) The bidirectional controlled ATHPF without source current or load current information is more suitable for the smart grid or microgrid with distributed nonlinear loads and distributed generation.
2) The ATHPF employing the bidirectional control principle attains a selective rather than global harmonic elimination with filtering performance independent of the deviation of passive filter parameters.
3) The bidirectional control principle can realize the flexible protection against harmonic over-current without losing harmonic elimination and reactive power compensation at the occurrence of harmonic over-current, whereby improving the operation reliability of ATHPF.
4) For three-phase ATHPF, the bidirectional control principle employs the split-phase independent control method with compensation performance immune to the filter parameters unbalance.

References

[1] D. Saxena, S. Bhaumik, and S. N. Singh, "Identification of multiple harmonic sources in power system using optimally placed voltage measurement devices," *IEEE Trans. Power Electron.*, vol. 61, no. 5, pp. 2483–2492, May 2014.

[2] P. Acuna, L. Moran, M. Rivera, J. Dixon, and J. Rodriguez, "Improved active power filter performance for renewable power generation systems," *IEEE Trans. Power Electron.*, vol. 29, no. 2, pp. 687–694, Feb. 2014.

[3] J. C. Das, "Passive filters-potentialities and limitations," *IEEE Trans. Ind. Appl.*, vol. 40, no. 1, pp. 232–241, Jan./Feb. 2004.

[4] H.-L. Jou, J.-C. Wu, Y.-J. Chang, and Y.-T. Feng, "A novel active power filter for harmonic suppression," *IEEE Trans. Power Del.*, vol. 20, no. 2, pp. 1507–1513, Apr. 2005.

[5] D. Rivas, L. Moran, J. W. Dixon, and J. R. Esinoza, "Improving passive filter compensation performance with active techniques," *IEEE Trans. Ind. Electron.*, vol. 50, no. 1, pp. 161–170, Feb. 2003.

[6] A. F. Zobaa, "Optimal multiobjective design of hybrid active power filters considering a distorted environment," *IEEE Trans. Ind. Electron.*, vol. 61, no. 1, pp. 107–114, Jan. 2014.

[7] B. Singh and V. Vishal "An indirect current control of hybrid power filter for varying loads," *IEEE Trans. Power Del.*, vol. 21, no. 1, pp. 178–184, Jan. 2006.

[8] S. P. Litran and P. Salmeron, "Reference voltage optimization of a hybrid filter for nonlinear load reference," *IEEE Trans. Ind. Electron.*, vol. 61, no. 6, pp. 2648–2654, Jun. 2014.

[9] P. Salmeron and S. P. Litran, "A control strategy for hybrid power filter to compensate four-wires three-phase systems," *IEEE Trans. Power Electron.*, vol. 25, no. 7, pp. 1923–1931, Jul. 2010.

[10] A. Bhattacharya, C. Chakraborty, and S. Bhattacharya, "Parallel-connected shunt hybrid active power filters operating at different switching frequencies for improved performance," *IEEE Trans. Ind. Electron.*, vol. 59, no. 11, pp. 4007–4019, Nov. 2012.

[11] M. A. Mulla, C. Rajagopalan, and A. Chowdhury, "Hardware implementation of series hybrid active power filter using a novel control strategy based on generalised instantaneous power theory," *IET Power Electron.*, vol. 6, no. 3, pp. 592–600, Mar. 2013.

[12] A. Hamadi, S. Rahmani, and K. Al-Haddad, "Digital control of a shunt hybrid power filter adopting a nonlinear control approach," *IEEE Trans. Ind. Informat.*, vol. 9, no. 4, pp. 2092–2104, Nov. 2013.

[13] S. Rahmani, A. Hamadi, K. Al-Haddad, and L. A. Dessaint, "A combination of shunt hybrid power filter and thyristor-controlled reactor for power quality," *IEEE Trans. Ind. Electron.*, vol. 61, no. 5, pp. 2152–2164, May 2014.

[14] Z. Shuai, A. Luo, J. Shen, and X. Wang, "Double closed-loop control method for injection-type hybrid active power filter," *IEEE Trans. Power Electron.*, vol. 26, no. 9, pp. 2393–2403, Sep. 2011.

[15] J. Gupta and A. Pati, "Improvement in the quality of load current by various controlling techniques in hybrid power filter for harmonic reference and resonance suppression," in *Proc. 2nd Int. Conf. Power Control Embedded Syst. (ICPCES)*, Allahabad, India, 2012, pp. 1–5.

[16] D. Detjen, J. Jacobs, R. W. De Doncker, and H. G. Mall, "A new hybrid filter to dampen resonances and compensate harmonic currents in industrial power system with power factor correction equipment," *IEEE Trans. Power Electron.*, vol. 16, no. 6, pp. 821–827, Nov. 2001.

[17] K. N. B. M. Hasan, K. Rauma, A. Luna, J. I. Candela, and P. Rodriguze, "Harmonic compensation analysis in offshore wind power plants using hybrid filters," *IEEE Trans. Ind. Appl.*, vol. 50, no. 3, pp. 2050–2060, May/Jun. 2014.

[18] R. Inzunza and H. Akagi, "A 6.6-kV transformerless shunt hybrid active filter for installation on a power distribution system," *IEEE Trans. Power Electron.*, vol. 20, no. 4, pp. 893–900, Jul. 2005.

[19] V. Verma and B. Singh, "Design and implementation of a current-controlled parallel hybrid power filter," *IEEE Trans. Ind. Appl.*, vol. 45, no. 5, pp. 1910–1917, Sep./Oct. 2009.

[20] V. F. Corasaniti, M. B. Barbieri, P. L. Arnera, and M. I. Valla, "Hybrid power filter to enhance power quality in a medium-voltage distribution network," *IEEE Trans. Ind. Electron.*, vol. 56, no. 8, pp. 2885–2893, Aug. 2009.

[21] G.-M. Lee, D.-C. Lee, and J.-K. Seok, "Control of series active power filters compensating for source voltage unbalance and current harmonics," *IEEE Trans. Ind. Electron.*, vol. 51, no. 1, pp. 132–139, Feb. 2004.

[22] S. H. Hosseini, T. Nouri, and M. Sabahi, "Power quality enhancement using a new hybrid active power filter under non-ideal source and load conditions," in *Proc. IEEE Power Energy Soc. Gen. Meeting (PES)*, Calgary, AB, Canada, 2009, pp. 1–6.

[23] G. A. Shah, V. C. Gungor, and O. B. Akan, "A cross-layer QoS-aware communication framework in cognitive radio sensor networks for smart grid applications," *IEEE Trans. Ind. Informat.*, vol. 9, no. 3, pp. 1477–1485, Aug. 2013.

[24] A. H. Etemadi, "Control and protection of multi-DER microgrids," Ph.D. dissertation, Dept. Elect. Comput. Eng., Univ. Toronto, Ottawa, Canada, 2012.

[25] Y. Deng and X. Tong, "Modeling and control strategy of active tuning hybrid power filter," in *Proc. IEEE Int. Asia-Pac. Power Energy Eng. Conf. (APPEEC)*, Shanghai, China, Mar. 2012, pp. 1–4.

[26] H. L. Ginn and L. S. Czarnecki, "An optimization based method for selection of resonant harmonic filter branch parameters," *IEEE Trans. Power Del.*, vol. 21, no. 3, pp. 1445–1451, Jul. 2006.

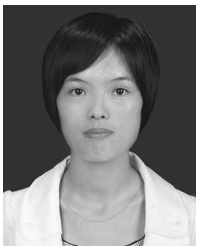

Yaping Deng was born in Shanxi Province, China, in 1984. She received the B.S. and M.S. degrees in electrical engineering from Xi'an University of Technology, Xi'an, China, in 2008 and 2011, respectively, where she is currently working toward the Ph.D. degree in electrical engineering.

Her research interests include analysis of power quality and control of hybrid power filter.

Xiangqian Tong was born in Shaanxi Province, China, in 1961. He received the B.S. degree from the Shaanxi Institute of Technology, Hanzhong, China, and the M.S. degree from Xi'an University of Technology, Xi'an, China, in 1983 and 1989, respectively, and the Ph.D. degree in electrical engineering from Xi'an Jiaotong University, Xi'an, in 2006.

He joined the Xi'an University of Technology in 1989. Since 2002, he has been a Professor and the Academic Leader of Electrical Engineering with the Xi'an University of Technology. His research interests include the application of power electronics in power system and control of power quality, especially the power filter, static synchronous compensator, and high voltage direct current.

Hao Jia was born in Shaanxi Province, China, in 1980. He received the B.S. degree in electrical engineering from Xi'an University of Technology, Xi'an, China, in 2008.

In 2012, he joined the Electrical Engineering Department, Xi'an University of Technology, where he is currently an Assistant Engineer. His research interests include application and digital control of power converters.